cambridge.org/lpb

Research Article

Cite this article: Mancelli D et al. (2025) Challenges of preliminary investigation of high repetition rate experiments enabling new paths on high energy density physics. Laser and Particle Beams 43, e5, 1–11. https://doi.org/10.1017/lpb.2025.10002

Received: 13 September 2024 Revised: 31 March 2025 Accepted: 14 May 2025

Keywords:

EOS; HED; HRR; SOP; VISAR; WDM

Corresponding author: Donaldi Mancelli; Email: dmancelli@hmu.gr

© The Author(s), 2025. Published by Cambridge University Press. This is an Open Access article, distributed under the terms of the Creative Commons Attribution licence (http://creativecommons.org/licenses/by/4.0), which permits unrestricted re-use, distribution and reproduction, provided the original article is properly cited.



Challenges of preliminary investigation of high repetition rate experiments enabling new paths on high energy density physics

Donaldi Mancelli^{1,2} , Alessandro Tentori³, Didier Raffestin³, Diluka Singappuli³, Jean-Marc Chevalier⁴, Oldrich Renner^{5,6}, Miroslav Krus⁵, Michal Krupka^{5,7}, Sushil Kumar Singh^{7,8,9} , Roman Dudzak^{5,7}, Shubham Agarwal^{7,10}, Gabriel Schaumann¹¹, Noaz Nissim¹², Yair Ferber¹², Eran Greenberg¹², Artem S. Martynenko¹³, Paul Neumayer¹³, Michael Tatarakis^{1,2}, Katarzyna Batani¹⁴ and Dimitri Batani³

¹Institute of Plasma Physics & Lasers, University Research & Innovation Centre, Hellenic Mediterranean University, Rethymno, Crete, Greece; ²Department of Electronic Engineering, School of Engineering, Hellenic Mediterranean University, Chania, Crete, Greece; ³University of Bordeaux, CNRS, CEA, CELIA, Talence, France; ⁴CEA, DAM, CESTA, Le Barp, France; ⁵Institute of Plasma Physics of the CAS, Prague, Czech Republic; ⁶The Extreme Light Infrastructure ERIC, ELI Beamlines Facility, Dolní Brezany, Czech Republic; ⁷Department of Radiation and Chemical Physics, FZU – Institute of Physics, Czech Academy of Sciences, Prague, Czech Republic; ⁸Laser-Plasma Department, Institute of Plasma Physics, Czech Academy of Sciences, Prague, Czech Republic; ⁹Department of Physics, Faculty of Electrical Engineering, Czech Technical University in Prague, Prague, Czech Republic; ¹⁰Department of Surface and Plasma Physics, Faculty of Mathematics and Physics, Charles University, Prague, Czech Republic; ¹¹Technische Universität Darmstadt, Institut für Kernphysik, Darmstadt, Germany; ¹²Applied Physics Division, Soreq NRC, Yavne, Israel; ¹³GSI Helmholtzzentrum für Schwerionenforschung GmbH, Darmstadt, Germany and ¹⁴Institute of Plasma Physics and Laser Microfusion (IPPLM), Warsaw, Poland

Abstract

In this work, we discuss the challenges related to the preliminary investigation of high repetition rate (HRR) experiments in the field of high energy density (HED) physics, and we present the results of preparation experiments done at the Prague Asterix Laser System (PALS) laser facility conducted with the aim of defining the needed developments in target design, real-time diagnostics and data collection needed to meet HRR requirements. Although the PALS laser facility is not an HRR facility, it has served as a valuable test bed for advancing diagnostic techniques and refining target design in preparation for HRR experimental platforms. HRR operation will result in improved statistical errors of the experimental results, in particular for experiments related to equation of state studies in extreme conditions.

Introduction

In recent years, new laser facilities have been developed that allow to deliver kJ-long pulses at repetition rates much higher than what was possible until the recent past (typically 1 laser shot/minute). Examples of such facilities are the L4n laser at ELI beamlines (Ref. 1), the DiPOLE100X at Eu-XFEL (Refs 2, 3), the Matter in Extreme Conditions (MEC) platform at LCLS (Refs 4, 5) and the high-energy/high-intensity laser facility PHELIX of the GSI (Refs 6, 7). Such facilities offer for the first time the possibility of performing high-energy density (HED) physics experiments (Ref. 8) at a high repetition rate (HRR). HED refers to conditions in which the energy density in matter exceeds $10^{11} \, \text{J/m}^3$ and pressures are above 1 Mbar (Ref. 8). Current large-scale laser facilities already allow accessing HED conditions, but the shot rate is very low going from 1 shot every 30 minutes (for instance, at PALS (Ref. 9)) to a typically one shot per day to MJ-scale facilities (like NIF (Ref. 10) or LMJ (Ref. 11)). Facilities operating at HRR will not only allow for more experimental results. They will also offer the possibility of attaining data with statistical significance, with error bars obtained from the standard deviation from several laser shots. This can open a new era in HED physics. We must specify that the HRR in the domain of HED refers to shot rate of the order of 1 minute today, possibly approaching 0.1 Hz to 1 Hz in the future. This is different from what is achieved with Petawatt (PW) short laser facilities which are currently operating at a repetition rate of several Hz and may achieve $\sim 100\,\mathrm{Hz}$ in the near future. In any case, the possibility of performing HRR experiments is not only related to laser performance. It requires the use of an adequate diagnostic system and target holders that will allow multiple shots. In

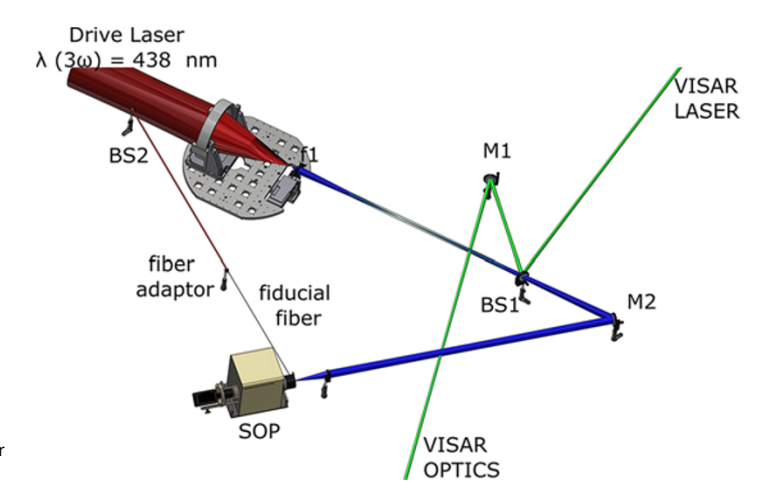


Figure 1. Experimental setup: the VISAR and SOP respectively measure the reflectivity and the self-emission of the shocked sample on the rear side to infer the shock velocity.

HED physics, diagnostics are used to measure and characterize the properties of matter under extreme conditions. They can provide information on various physical quantities, including temperature, density, pressure and the equation of state (EOS) of the material (Refs 12, 13). Overall, diagnostics play a critical role in HED physics experiments by providing the data needed to understand the behaviour of matter in extreme conditions (Refs 14, 15). As technology continues to advance, new and more sophisticated diagnostic techniques will continue to be developed, enabling researchers to gain deeper insights into the properties of matter at the extremes of pressure, temperature and density.

Although many diagnostics have been extensively used on low repetition rate experimental platforms, their suitability for HRR operation must be investigated (Ref. 16).

In addition, the target requirements are also different: HRR operation implies the need for positioning and aligning the target also at HRR using a dedicated motorized target holders, but it also implies that a laser shot on a given target will not affect, damage or even destroy the targets to be shot afterwards. A characterization of the debris emitted by the target is also needed, in view of the protection of the targets, the diagnostic and the laser optics themselves.

In this context, we conducted an experimental campaign at the PALS (Ref. 9) laser facility to explore the challenges related to HRR operation. Although PALS is a single-shot low repetition rate facility (allowing 1 shot every ~30 min), several questions related to the preparatory study of HRR experiments can also be studied here. Development of a target holder compatible with HRR requirements and debris mitigation were among the main challenges investigated in the campaign. At the same time, this campaign has offered the possibility of implementing new diagnostic tools which were previously not available in the facility, such as Shock Chronometry (SOP), Velocity Interferometry System for any Reflector (VISAR) and Photon Doppler Velocimetry (PDV) which will also be described in this paper.

Experimental setup

PALS laser facility

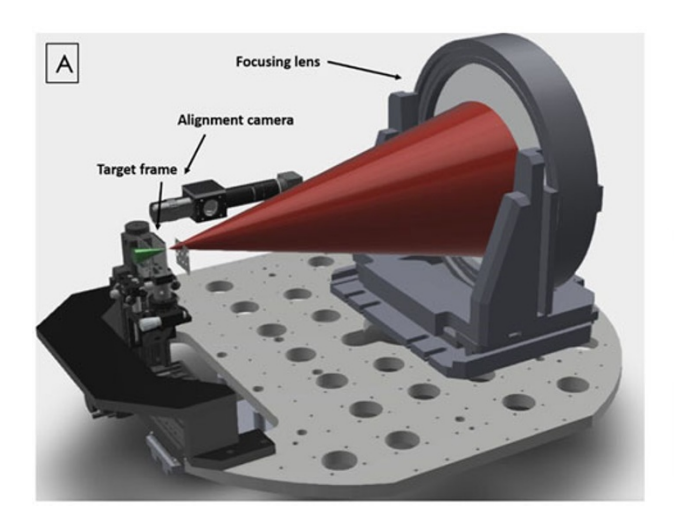
The iodine laser facility PALS (Ref. 9) can deliver energy in exam of 200 J with pulse duration of 250 ps full width at half maximum (FWHM) at the third harmonic ($\lambda_{3\omega}=438$ nm). The beam was focused to a 400 μ m FWHM focal spot on target using

phase-plate, giving an intensity of $\sim 10^{14} \rm W/cm^2$. We utilized multi-layer targets consisting of 10 $\mu \rm m$ CH, 400 nm Au and 100 $\mu \rm m$ SiO $_2$ of dimensions $1.4\times1.4~\rm mm^2$ supported by aluminium frames. The design of the experimental setup is shown in Figure 1. Target frames and alignment cameras were mounted separately on a three-axis motion system as shown in Figure 2.

Experimental setup - target design

So far targets for low repetition rate HED experiments are designed individually and individually aligned. However, HRR facilities have to overcome this barrier and use targets which are compatible with HRR operation. One simple design consists of the large-framed sample as shown in Figure 2A and B, with motorized three or more axis motion system with $\mu \rm m$ accuracy and user-friendly control system.

In our experiment, the targets and target frame were designed and fabricated by Technische Universität Darmstadt (TUDa). Frame dimensions, the number of targets per frame and distances between targets are of primary importance. These parameters must be fine-tuned and need to be adapted for each experiment, according to the actual target characteristics and laser parameters. In our experimental campaign, each frame contained nine targets which were shot in a row without breaking the vacuum in order to simulate the conditions similar to HRR as shown in Figure 3. The frame contains alignment markers for target positioning. Each target is prepared separately and installed inside a hole in the frame, protecting neighbouring targets from debris ejected after the laser shot both in the forward and backward direction. Several target frames containing 3×3 targets with different designs have been tested in the experimental campaign at the PALS laser facility. The targets are separated by a distance of 12 mm, which was found to be sufficient to avoid damage to neighbouring targets from the shock propagating along the frame when firing a specific target. Figure 4 shows target frames with orthogonal and circular openings for the laser cone. The distance between individual targets might have to be scaled with laser energy. A compromise between a safe distance between targets and a large number of targets per frame is essential to ensure compatibility with HRR experiments. The entire target alignment process is based on software developed in Python programming language. The concept, motion control software and user interface were implemented and tested by the target laboratory of TUDa.



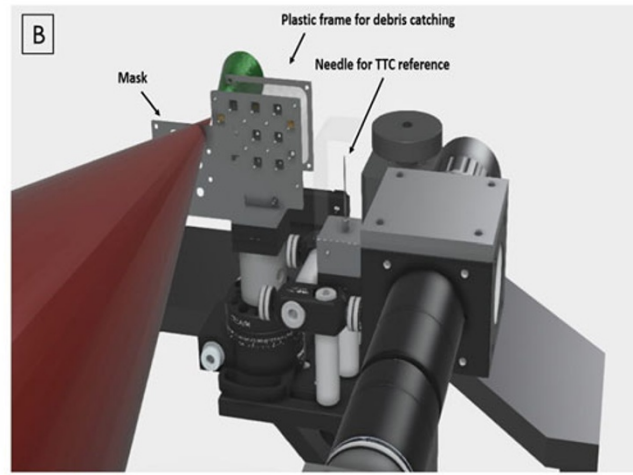
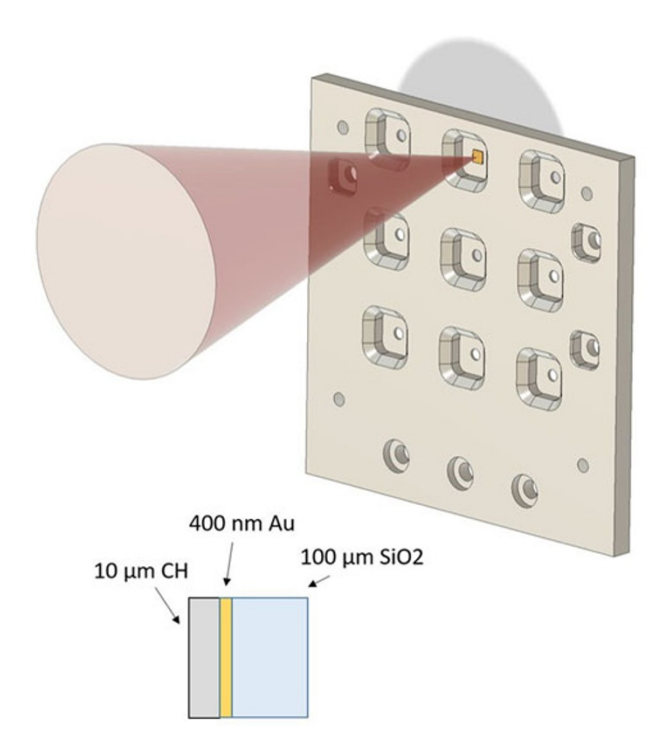


Figure 2. CAD design of details of the interaction chamber showing the target manipulator along with the alignment camera and the needle required for referencing the target chamber center (TCC). Red cone represents the converging laser beam at the third harmonic.



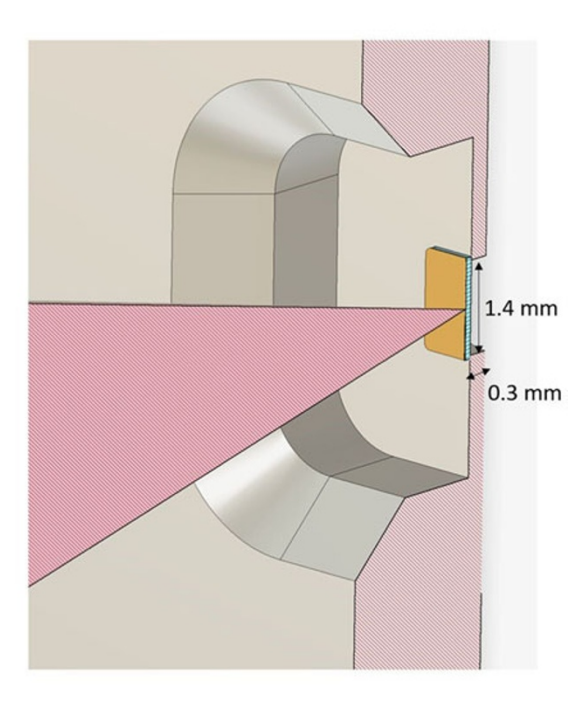


Figure 3. Conceptual design of the aluminium-framed target to be used with the detailed layer thicknesses and the laser cone. In the projected cut of the proposed design, we show details on the height of the target and the thickness of the base-plate of the frame where the targets are glued.

Raw-data formatting

Development and commissioning of HRR facilities also need the implementation of new data formatting standards to assist real-time data handling and analysis, providing feedback during and experimental campaign. For instance, raw data produced on HRR facilities can be stored in hierarchical format HDF5 (Ref. 17) that allow managing very large data file format of the order of $\sim\!100\,\mathrm{GB}$. The HDF5 format is also applied to several hydro and particle in cell codes as well (e.g. FLASH MHD code (Refs 18–22), SMILEI (Ref. 23), EPOCH (Ref. 24), etc.) due to its versatile features. The advantages and some key parameters of HDF5 format are the following:

- Efficient Storage and Access: HDF5 is designed to handle large amounts of data efficiently. Supports chunking and compression, which can significantly reduce file size and improve I/O performance.
- (2) Portability: HDF5 files are platform-independent, ensuring that data can be shared and accessed across different computing environments without compatibility issues (conventional computer to high-performance computing (HPC) systems).
- (3) Scalability: HDF5 can manage datasets that are too large to fit into memory, making it suitable for HPC applications.
- (4) Metadata Support: HDF5 supports the storage of rich metadata alongside the actual data. This can include information

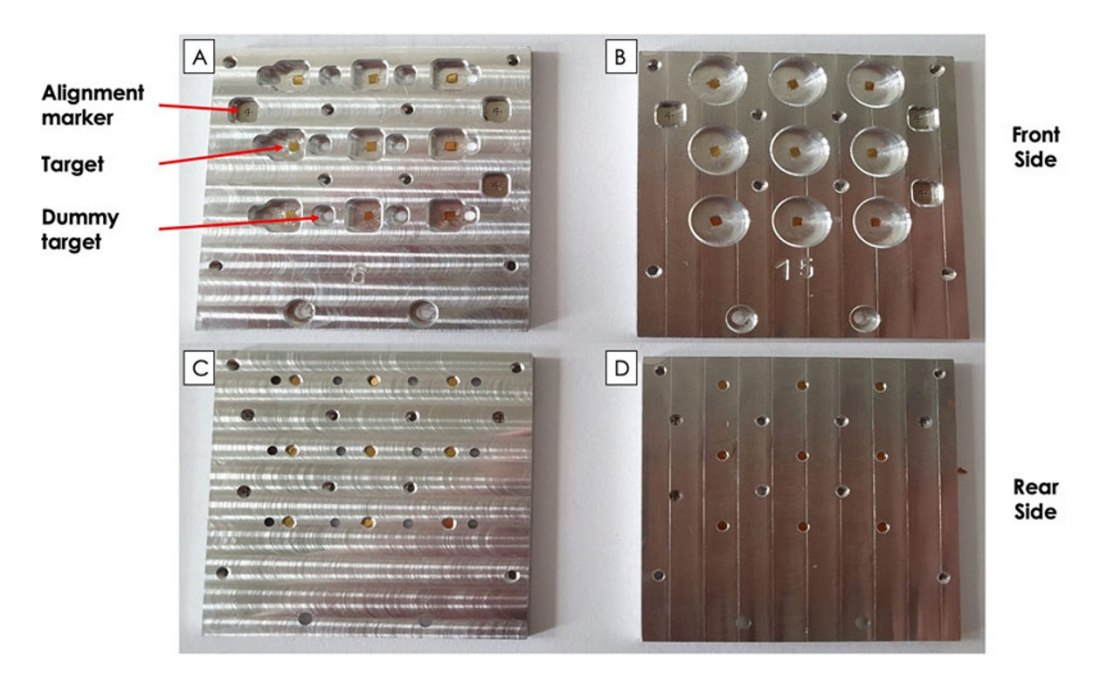


Figure 4. A and C framed target with rectangular opening, and in the second column B and D, the frame with circular openings. In both cases, the frames included dummy targets, alignment markers and the multi-layered sample of interest.

- about the origin, structure and the meaning of data, which is essential for data analysis and reproducibility.
- (5) Compatibility with Multiple Programming Languages: HDF5 has APIs for various programming languages, including C, C++, Fortran, Python and Java, being accessible to a wide range of developers and researchers.
- (6) Parallel I/O: HDF5 supports parallel I/O operations, enabling efficient data read/write operations in HPC environments.
- (7) Community and Support: HDF5 has a strong user community and extensive documentation, helping users troubleshoot issues.

Overall, HDF5 is a powerful tool for managing complex data in scientific computing, engineering and various data-intensive applications, providing both flexibility and efficiency in data storage and retrieval. Data handling and storing can be further assisted with modern tools and algorithms by machine learning and maybe using AI. HDF5 format is a standard format for many research facilities around the world including large-scale laser facilities (OMEGA at LLE, users can access the diagnostics data database after the experiment) and research centres not related to laser plasma such us particle accelerators CERN or GSI FAIR, where big data are produced, stored and made available in real time to researchers.

Debris characterization

Debris production is a common issue in HED physics experiments that can affect the accuracy of measurements and damage experimental equipment. Debris can be generated by a variety of processes. Typical results of debris generated from multilayered planar targets irradiated under different laser drive conditions are presented in Figure 5. Several types of debris can be generated during HED physics experiments, including:

- Plasma debris, which is generated by the ablation of the target material and the interaction of laser light with the target. Plasma debris can interfere with measurements by scattering or absorbing light and can also cause damage to experimental equipment by depositing energy in unwanted locations.
- Solid debris, which is generated by fragmentation of the target material due to compression and heating, as shown in Figure 5. Solid debris can damage experimental equipment by impacting and scratching surfaces. Debris is also generated by the interaction of high-energy particles with the target material. These can cause damage to experimental equipment by depositing energy in unwanted locations and can also be a safety hazard for researchers.

There are several methods for mitigating the effects of debris in HED physics experiments. Shielding can be used to protect experimental equipment from debris by placing a barrier between the target and the equipment. For instance, in future experimental campaign pre-pulses can be used to reduce the amount of plasma debris generated during an experiment by ablating some of the target material before the main laser pulse. The target design can be optimized to minimize the amount of debris generated during an experiment. For example, targets can be designed with a smooth surface to reduce fragmentation or with multi-layers structured to reduce plasma debris. Diagnostic design can be optimized to minimize the effects of debris on measurements. For example, diagnostic equipment can be placed in a way that minimizes the amount of debris that reaches it. Also a motorized tapes acting as debris shield can be implemented on HRR facilities or a largeframed shield holder coupled to the target frame can be used as an alternative option. Future work should investigate the cumulative effects of debris on optical components and target alignment reliability over multiple consecutive shots in HRR conditions (1-10 Hz).

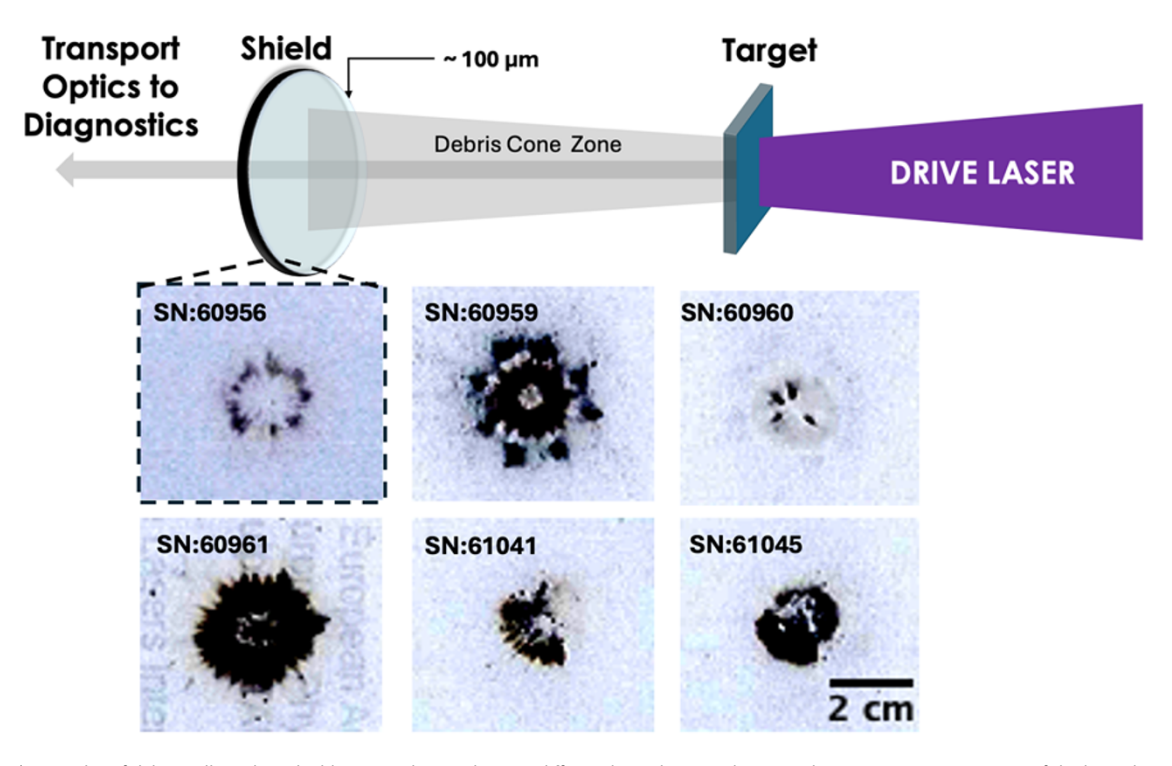


Figure 5. (Top) Examples of debris collected on shield in several PALS shots, at different laser drive conditions and target composition. Setup of the laser drive, target and debris shield in planar geometry. The distance between target and shied is \sim 4 cm. High-quality transparent plastic debris shields were used and replaced after each shot. (Bottom) Six representative debris shield scans are presented for different laser energies and target configurations. These include 25 μ m Al foils used in shots (#60956-#60961) at laser energies of 151.8, 118.7, 51 and 165 J, as well as stepped targets for shot #61041 (10 μ m CH/10 μ m Al base/ 33 μ m Al step/51 μ m BN step) and shot #61045, with laser energies of 112 and 133 J, respectively.

Diagnostics

The development of a precise diagnostic for HED physics in HRR conditions is crucial for understanding fundamental physics (Refs 25–28). Diagnostic approaches suitable for HRR operation can be divided in three groups as follows: of course, to work in HRR, these diagnostics must be coupled to active detectors, e.g. replacing films with multi-channel plates detectors.

(1) Optical diagnostics

- Interferometry: Provides electron density profiles by measuring the phase shift of light passing through plasma (Refs 29, 30).
- Schlieren and Shadowgraphy can provide researchers with images that contain information on the density gradient in the plasma (Refs 30, 31).
- Thomson Scattering: Offers detailed measurements of electron temperature and velocity distribution by measuring the scattering of light-produced plasma electrons (Ref. 32).
- Optical Emission: Capture time-resolved optical emissions (e.g. using streak cameras), providing images or spectra to get insights into the temporal evolution of plasma (Refs 33, 34).

(2) X-ray Diagnostics

- X-ray radiography: uses X-rays to image dense plasmas, revealing density structures and ablation processes in ICF targets (Refs 35–37). Recent developments include the use of X-ray Phase Contrast imaging (Ref. 38).
- X-ray emission spectroscopy: Analyses energetic, temporal and spatial distribution of X-ray emission (including freefree, free-bound and bound-bound electron transitions)

- to study energy deposition in targets and determine the macroscopic parameters of the ionized matter (in particular electron and ion temperature, density and particle velocity distribution) and processes occurring in the plasma. Techniques like $K\alpha$ and L-shell emission spectroscopy are commonly used (Refs 39, 40).
- X-ray Imaging: Pinhole cameras, Kirkpatrick-Baez (KB) microscopes and imagers based on diffraction of X-rays from 2D-bent crystals are used to create detailed images of plasma, providing spatial resolution of hot spots and other features (Refs 41, 42).

(3) Particle Diagnostics

- Charged Particle Spectroscopy: Measures the energy and distribution of ions and electrons, providing information on acceleration mechanisms and energy transfer (Refs 43–45).
- Neutron Diagnostics: Detects neutrons produced in fusion reactions, offering insights into reaction rates and fuel conditions in fusion experiments (Ref. 46).

Each of these diagnostics provides unique insights into different aspects of plasmas created by high-energy lasers, making them essential tools for advancing our understanding of these complex systems. In the following, we will just focus on the use of optical diagnostics related to studies of shock waves and EoS experiment (VISAR, SOP and PDV). These are indeed examples of diagnostics, which are employed frequently in HED physics experiments, and which provide online and real-time detection, therefore they are suited for HRR operation. Indeed, these are the diagnostics developments which we have introduced

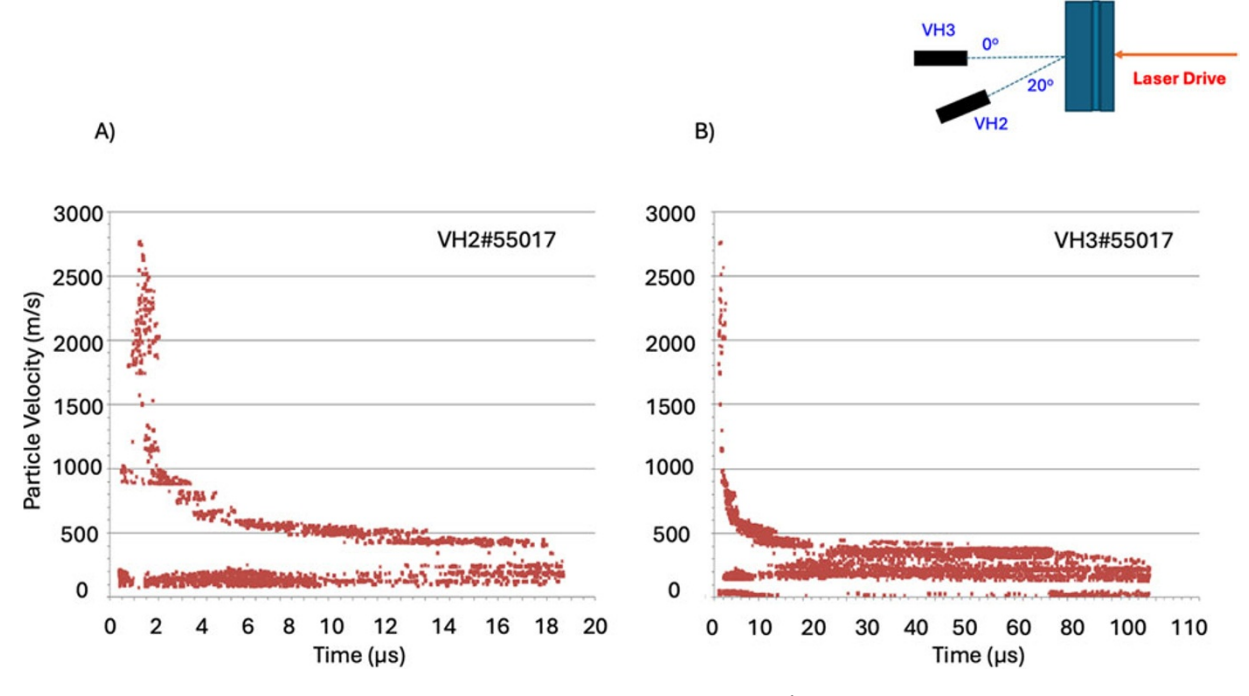


Figure 6. Results from PDV for shot #55017 for target CH/Au/SiO₂ the laser intensity was $\approx 3 \times 10^{14} \mathrm{W/cm^2}$ on target with the fibres placed to look at two different angles 0° (A), and 20° (B), respectively.

at the PALS laser facility in the framework of the present work.

Shock diagnostics - PDV

PDV is a diagnostic technique commonly used in fluid dynamics, shock physics and material science to measure velocity profiles and shock velocities in high-speed events. It is a non-intrusive method that relies on the Doppler shift of light to determine velocities. PDV is a fibre-based diagnostic suited for the extreme conditions created by high-speed impact, explosives, pulsed power machines such us Z-pinch (Refs 47-49) or X-pinch devices (Ref. 50) and in high-power laser-matter interactions. PDV is a heterodyne laser interferometry that operates on the principle of the Doppler effect. A probe beam is sent to the surface of the target of interest. A portion of the reflected light is collected together and interferes with the incoming probe light in a sensors, usually a photo-diode or a photomultiplier tube. As the target moves, the reflected light undergoes a frequency shift proportional to the target velocity, which produces a beating with the incoming (unshifted) light. This allows the frequency shift to be detected by the sensor and using short-time Fourier transform algorithm and the Doppler equation, PDV can measure velocities of reflecting surface (or reflecting particles) with high precision (Refs 51, 52).

PDV is a compact diagnostic, suitable for laser–matter interaction, which can be adapted to HRR experiments (Ref. 53), and gives valuable information about high-speed phenomena without disturbing the system under study. Some indicative cases are listed below:

- Shock Physics: PDV is used to measure shock velocities and study the propagation of shock waves in materials.
- Fluid Dynamics: It helps characterize the flow of fluids in highspeed events such as explosions or impacts.

 Material Science: PDV is used to study the behaviour of materials under extreme conditions, such as high pressure or temperatures.

From the data collected by the fast detector, it is also possible to get accurate values for the shock breakout times. This can be done by measuring the signal on the same scope as a timing fiducial (e.g. a reflection of the drive-laser). Using short-time Fourier analysis procedure on the obtained PDV signal, we obtain a spectrogram.

From this we can obtain shock velocities in transparent materials or either free-surface velocity or the velocity of the debris ejected from the shocked sample. Since the PDV imaging lens attached to the fibre typically collects data from a small region of the sample (in an area of $< 100 \,\mu\mathrm{m}$ diameter), this makes it ideal for stepped targets, where multiple probe fibres can be set on the rear side of the target and at different angles, hence probing deferent regions were particle population can be different. Figure 6 shows the fast particle population obtained from two probes placed at different angles 0° and 20° for the multilayered planar target. In Figure 6A at early times $(0 - 4 \mu s)$, we observe a population of fast particles with high particle velocity $>> 500 \,\mathrm{ms^{-1}}$. These fast particles quickly leave the field of observation. At later times $> (4 \mu s)$, we observe two distinct populations of particles in free flight with velocities of ~ 500 and $\sim 150 \, \mathrm{ms^{-1}}$. On the other hand at 20° (Figure 6B), and at times $> 20 \,\mu$ s, one can observe a large population of particles with velocities on the order of 400 ms⁻¹, and a lower population of particles with high velocity. For the plasma, the typical expansion takes place at 10⁵ ms⁻¹ (for a temperature of the order of a few hundreds eV). However, the plasma recombines and vanishes more quickly while the particle debris can travel in free flight to larger distances.

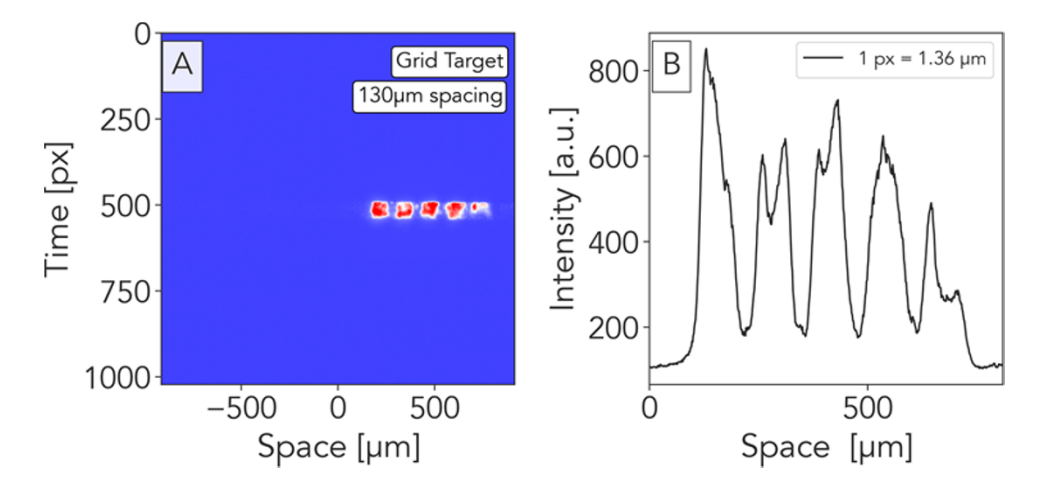


Figure 7. Grid test target was placed at TCC to optimize the SOP collection optics line and measure the extension of the field of view and spatial resolution. The separation of the cells is $130 \, \mu m$.

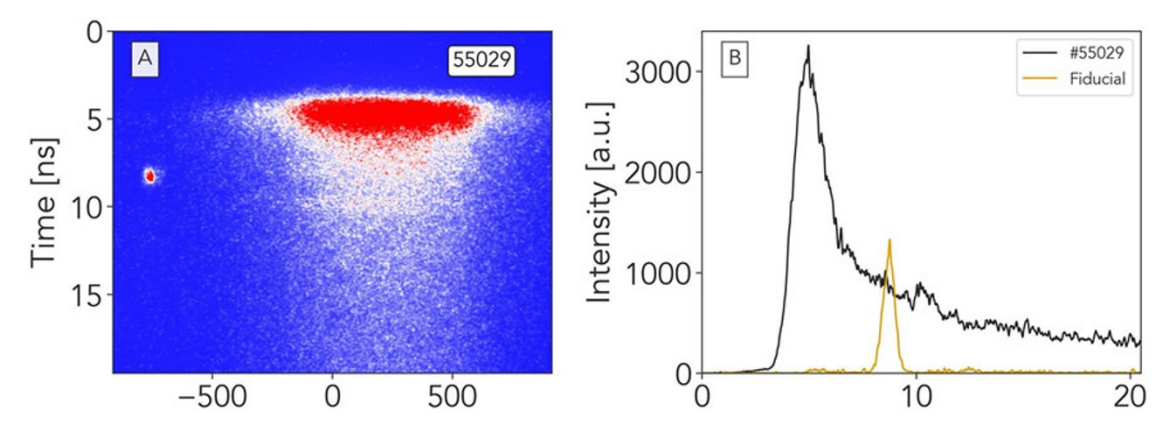


Figure 8. SOP results: (A) Self-emission from the rear side of a shocked target ($10 \, \mu \text{m}$ CH/ $0.4 \, \mu \text{m}$ Au/ $100 \, \mu \text{m}$ SiO₂). The small signal on the left is a time fiducial taken from the interaction beam, (B) line out of the previous image (shot #55029), with laser energy 113 J at 3ω giving an intensity of the order of ($3.6 \times 10^{14} \text{W cm}^{-2}$).

Shock diagnostics - SOP

VISAR and SOP have been widely used in laser-shock experiments, and their combination can provide the spatial and temporal evolution of hydrodynamic parameters related to the shock propagation in the target. The optical line used in our experiment at PALS experiment for SOP and VISAR is shown in Figure 1. The field of view of diagnostics and spatial resolution can be measured by placing a grid on the target chamber centre and shine with an alignment HeNe laser. The result is shown in Figure 7A with a line out taken from raw data in Figure 7B. This results in field of view (active observable area) of the order of \sim 750 μ m. Multiple imaging optical configurations were utilized and evaluated. The first configuration used a doublet achromat as the main imaging lens referred to as f1 in Figure 1. In the second configuration, we replaced the f1 lens with a photographic objective (Tamron 1:1,8 f=50 mm), which yielded a better imaging quality. A two-lens system was employed to capture the shock break out signal and direct it into a Hamamatsu Streak camera working in the visible range.

Typical shock emission signal obtained from SOP is shown in Figure 8. The drive parameters for shot #55029 for CH/Au/SiO $_2$ target, irradiated at 3ω light, with energy 113 J giving an intensity on target $3.6\times10^{14} \rm W~cm^{-2}$. The sweep window on the streak was set at 20 ns and the slit width was of the order of 150 μm . Notice that

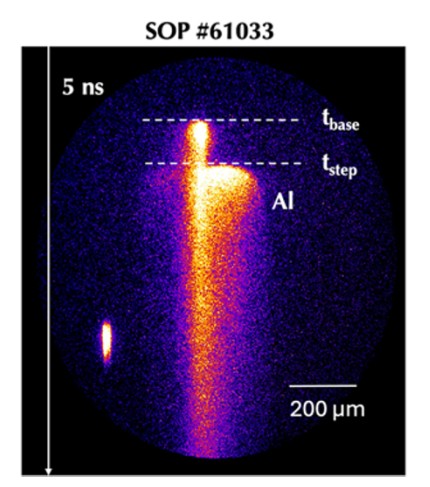
in case transparent materials are used as ablators, it is advisable to put a very thin opaque layer ($\leq 100 \, \mathrm{nm}$ of aluminium or carbon) to avoid the effect of laser shine-through.

Finally, Figure 9A shows the SOP image obtained by focusing the laser beam on an Al-stepped target. The target included a 10 μm CH foil (with anti shine-through layer, 200 nm) followed by a 10 μm Al base and a 38 μm Al step. In the SOP image, the shock breakout at the base and the shock breakout at the step are clearly visible. This configuration is often used in laser-driven shock-EOS experiments, where Al is often used as a reference material (Refs 54, 55). Since the thickness of the step is known, the results from SOP allow one to obtain the average shock velocity in the step. In the case of stationary shocks, this allows recovering all the thermodynamical quantities of Al by knowing its Hugoniot curve.

Shock diagnostics - VISAR

VISAR is a velocity interferometer that measures the velocity of a reflective surface by measuring the Doppler effect induced on a probe laser beam that illuminates this moving surface. It has been introduced by researchers from Los Alamos, and later it has been mainly used for experiments relative to laser-driven shock and studies of materials at extreme pressures. VISAR is based on

A) B)



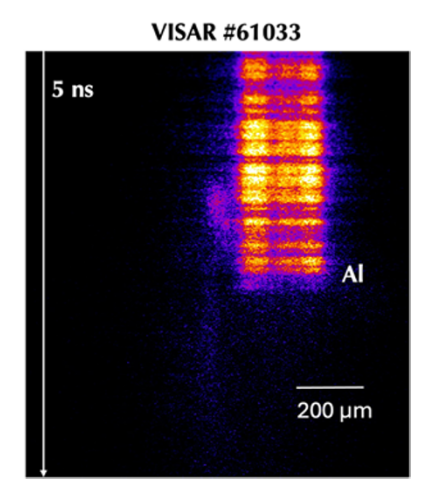


Figure 9. (A) Typical SOP image of shock breakout from the stepped target (shot PALS #61033), horizontal dashed lines indicate the break out time in base (t_{base}) and in the step (t_{step}) of the sample. **(B)** Typical reflectivity image obtained from VISAR, for the same stepped sample. Strong signal of reflectivity is observed from the Al step up to breakout time.

the Mach-Zehnder interferometer coupled to a streak camera to obtain a time-resolved measurement (Refs 56-60). At PALS, we implemented a system based on 2-inch optics which used a green laser system at 527 nm as source of the probe VISAR beam. The duration of such laser pulse could be adjusted from 50 to 320 ns. During the initial stage, we begin the alignment and optimization of VISAR setup with an energy of around 4 mJ and a pulse duration of approximately 50 ns FWHM. At the maximum power level, we used a pulse energy of (18.0 \pm 0.2) mJ with a FWHM duration of 320 \pm 10 ns. These are the input settings for the VISAR laser probe, specifically for the first mirror of the optical setup. In this experiment, the system was only used as a reflectivity diagnostics (i.e. one of the two arms of the interferometer is cut out). Figure 9B shows the reflectivity image obtained from the same shot of the SOP image in Figure 9A. We see on the right of the image the reflection from the surface of the Al step, which suddenly stops when the shock breaks out from Al rear surface. The reflection from the Al base was weak due to a problem in surface reflectivity of this target (and significant surface roughness). The horizontal intensity spikes are due to the beating between the different modes of the probe laser (not a single mode laser).

Both the VISAR and SOP systems used the same objective lens, namely the Tamron 1:1,8 f=50 mm lens. Outside the vacuum chamber (60 cm from the objective), we positioned a dichroic mirror. This mirror had the purpose of reflecting the green probe beam emitted by the VISAR probe, while simultaneously allowing the remaining emitted light for the SOP system to pass through. The beam was subsequently sent to a Mach–Zehnder interferometer with 2-inch optics and then directed by set of mirrors and lenses to the slit of an Optronis Optical streak camera with S20 photocathode sensitive to visible range.

Hydro simulation

To interpret our experimental results, we performed 1D radiative hydrodynamic simulations with the code MULTI (Ref. 61). The laser pulse was Gaussian in time with a plateau duration of 250 ps at FWHM at 3ω . A set of SESAME tables was used to perform the hydrodynamic simulations: table 7770 of parylene, SESAME table 2700 for gold and SESAME 7385 for quartz (Ref. 62). Tabulated EOS for different materials can be generated

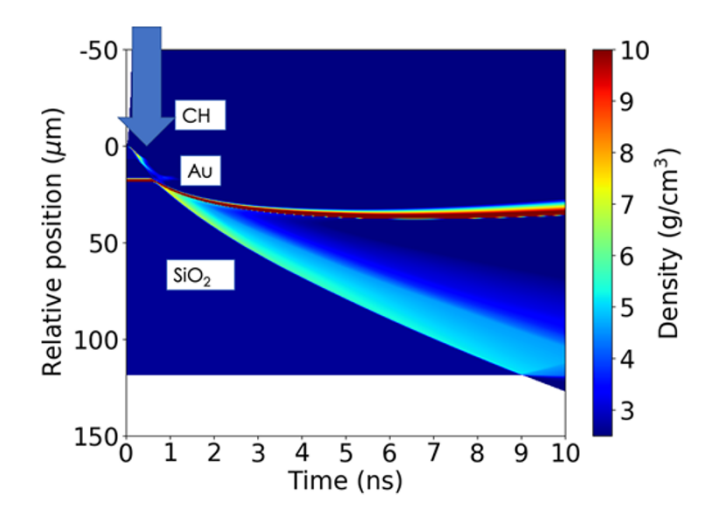


Figure 10. Density map from radiative hydrodynamic simulations using the MULTI code. Simulation indicates shock breakout at the gold–quartz interface at 0.65 ns. The target and laser parameters were the same as the ones stated in Section 2.

using quotidian equation of state (Ref. 63) and an updated version of it FEOS in SESAME format and PrOpacEOS (Ref. 64) code as well. The target thicknesses were $10\,\mu m$ CH $-0.4\,\mu m$ Au $-100\,\mu m$ SiO2. Figure 10 shows the density map reproducing the shot #55029. We see a shock breakout in the gold/SiO2 interface at 0.65 ns. This is compatible with the breakout time observed on SOP signal.

Several similar hydrodynamic simulations codes are extensively used by the laser plasma-community (e.g. 1D MULTI (Ref. 61), LILAC (Ref. 65), ESTER (Ref. 66), HYADES (Ref. 67), etc.).

Although such 1D hydro are quite fast, in order to allow their use in real time could be possible to combine them with physics-assisted machine learning methods combined with genetic algorithm's. This method could also be implemented and coupled to 2D or 3D hydro codes such as MULTI-2D (Ref. 68) and FLASH code (Refs 19–22), which on the other hand require more computational time as well. Such codes will provide valuable information on the planarity of the shock wave that is moving through the sample. Moreover, physics-assisted machine-learning is also necessary for

handling large amount of data that are generated from such simulations on large HPC systems and from the HRR experiments. While AI and machine-learning offer potential for HRR diagnostic development and simulation codes, their application and validation are still pending, as for this study we do not present such results since it was not the main focus of this experimental campaign. Finally, they could assist with the interpretation of the diagnostics results (Ref. 69).

Conclusions

In this paper, we presented some of the technical challenges related to the development of HRR experimental platforms for HED physics using high-power laser facilities. Such facilities (e.g. L4n ELI beam lines) may open new perspectives in HED science which were not accessible using low-repetition-rate facilities. They may allow getting increased sets of data with statistical significance. New development pathways must be addressed to facilitate the needs of the HRR facility in terms of targets, safety, simulation codes, diagnostics, data handling and analysis in real time. Future work will need expertise from both inside and outside the laserplasma community to improve and use these techniques in experiments. We will also need to identify specific scientific goals that novel approaches can achieve in the field of HRR science. In future experimental campaigns, further validation under real HRR conditions, with consecutive shots at high frequency (e.g. 1-10 Hz), will be necessary to confirm the suitability of VISAR, SOP and PDV for

Acknowledgements. We would like to acknowledge financial support from the LASERLAB-EUROPE Access to Research Infrastructure activity within the EC's Seventh Framework Program (No. 871124). We would like to acknowledge that Donaldi Mancelli was funded by the Hellenic Mediterranean University within the project 'Proposal for post-doctoral research at the Institute of Plasma Physics and Lasers (IPPL) of Hellenic Mediterranean University (HMU)' in the context of the 2607/Φ.120/04-05-2022 call of HMU for post-doctoral research. The work of A.S. Martynenko was supported by the Alexander von Humboldt Foundation. The involved teams have operated within the framework of the Enabling Research Project: ENR IFE.01.CEA, 'Advancing shock ignition for direct-drive inertial fusion'. We acknowledge that targets and target frames were designed and fabricated by Technische Universität Darmstadt (TUDa). This research work was also supported by the Ministry of Youth and Sports of the Czech Republic (Project No. LM2023068 and LM2018114 (PALS RI)). Finally, we thank the technical staff of PALS for their help in running the experiments.

References

- Jourdain N, Chaulagain U, Havlík M, Kramer D, Kumar D, Majerová I, Tikhonchuk VT, Korn G and Weber S (2020) The L4n laser beamline of the P3-installation: Towards high-repetition rate high-energy density physics at ELI-Beamlines. Matter and Radiation at Extremes 6, 015401.
- Mason P, Banerjee S, Smith J, Butcher T, Phillips J, Höppner H, Möller D, Ertel K, De Vido M and Hollingham I (2018) Development of a 100 J, 10 Hz laser for compression experiments at the high energy density instrument at the European XFEL. High Power Laser Science and Engineering 6, e65.
- Banerjee S, Mason P, Phillips J, Smith J, Butcher T, Spear J, De Vido M, Quinn G, Clarke D and Ertel K (2020) Pushing the boundaries of diodepumped solid-state lasers for high-energy applications. *High Power Laser Science and Engineering* 8, e20.
- 4. Nagler B, Arnold B, Bouchard G, Boyce RF, Boyce RM, Callen A, Campell M, Curiel R, Galtier E, Garofoli J, Granados E, Hastings J, Hays G, Heimann P, Lee RW, Milathianaki D, Plummer L, Schropp A, Wallace A, Welch M, White W, Xing Z, Yin J, Young J, Zastrau U and

- **Lee HJ** (2015) The matter in extreme conditions instrument at the linac coherent light source. *Journal of Synchrotron Radiation* **22**, 520–525.
- 5. Glenzer SH, L B Fletcher, Galtier E, Nagler B, Alonso-Mori R, Barbrel B, Brown SB, Chapman DA, Chen Z, Curry CB, Fiuza F, Gamboa E, Gauthier M, Gericke DO, Gleason A, Goede S, Granados E, Heimann P, Kim J, Kraus D, MacDonald MJ, Mackinnon AJ, Mishra R, Ravasio A, Roedel C, Sperling P, Schumaker W, Tsui YY, Vorberger J, Zastrau U, Fry A, White WE, Hasting JB, Lee HJ (2016) Matter under extreme conditions experiments at the linac coherent light source. Journal of Physics B: Atomic, Molecular and Optical Physics 49, 092001.
- 6. Bagnoud V, Aurand B, Blazevic A, Borneis S, Bruske C, Ecker B, Eisenbarth U, Fils J, Frank A, Gaul E, Goette S, Haefner C, Hahn T, Harres K, Heuck H-M, Hochhaus D, Hoffmann DHH, Javorková D, Kluge H-J, Kuehl T, Kunzer S, Kreutz M, Merz-Mantwill T, Neumayer P, Onkels E, Reemts D, Rosmej O, Roth M, Stoehlker T, Tauschwitz A, Zielbauer B, Zimmer D and Witte K (2010) Commissioning and early experiments of the PHELIX facility. Applied Physics B 100, 137–150.
- Zs. Major UE, Zielbauer B, Brabetz C, Ohland JB, Zobus Y, Roeder S, Reemts D, Kunzer S and Götte S (2024) High-energy laser facility PHELIX at GSI: latest advances and extended capabilities. *High Power Laser Science and Engineering* 12, e39.
- 8. Drake RP (2010) High-energy-density physics. Physics Today 63, 28-33.
- Jungwirth K, Cejnarova A, Juha L, Kralikova B, Krasa J, Krousky E, Krupickova P, Laska L, Masek K, Mocek T, Pfeifer M, Präg A, Renner O, Rohlena K, Rus B, Skala J, Straka P and Ullschmied J (2001) The Prague asterix laser system. *Physics of Plasmas* 8, 2495–2501.
- Miller GH, Moses EI and Wuest CR (2004) The national ignition facility: enabling fusion ignition for the 21st century. Nuclear Fusion 44, S228.
- Miquel J-L, Batani D and Blanchot N (2020) Overview of the laser mega joule (LMJ) facility and PETAL project in France. The Review of Laser Engineering 42, 131.
- 12. Mancelli D, Errea I, Tentori A, Turianska O, Larreur H, Katagiri K, Ozaki N, Kamimura N, Kamibayashi D, and Ishida K (2021) Shock Hugoniot data for water up to 5 mbar obtained with quartz standard at high-energy laser facilities. Laser and Particle Beams Volume 2021 2021 e2.
- 13. Zhang H, Yang Y, Yang W, Guan Z, Duan X, Yang M, Liu Y, Shen J, Batani K, Singappuli D, Lan K, Yongsheng L, Huo W, Liu H, Yulong L, Yang D, Sanwei L, Wang Z, Yang J, Zhao Z, Zhang W, Sun L, Kang W and Batani D (2024) Equation of state for boron nitride along the principal Hugoniot to 16 Mbar. Matter and Radiation at Extremes 9, 057403.
- Batani D (2016) Matter in extreme conditions produced by lasers. *Europhysics Letters* 114, 65001.
- 15. Hye-Sook Park SJMA, Celliers PM, Coppari F, Eggert J, Krygier A, Lazicki AE, Mcnaney JM, Millot M, Ping Y, Rudd RE, Remington BA, Sio H, Smith RF, Knudson MD and McBride EE (2021) Techniques for studying materials under extreme states of high energy density compression. *Physics of Plasmas* 28, 060901
- 16. Batani D, Colaïtis A, Consoli F, Danson CN, Gizzi LA, Honrubia J, Kühl T, Pape SL, Miquel J-L and Perlado JM (2023) Future for inertial-fusion energy in Europe: a roadmap. High Power Laser Science and Engineering 11, e83.
- For more information on HDF5, visit: https://www.hdfgroup.org/solutions/hdf5/.
- Dubey A, Antypas K, Ganapathy MK, Reid LB, Riley K, Sheeler D, Siegel A and Weide K (2009) Extensible component-based architecture for flash, a massively parallel, multiphysics simulation code. *Parallel Computing* 35, 512–522.
- Fryxell B, Olson K, Ricker P, Timmes FX, Zingale M, Lamb DQ, MacNeice P, Rosner R, Truran JW and Tufo H (2000) Flash: An adaptive mesh hydrodynamics code for modeling astrophysical thermonuclear flashes. The Astrophysical Journal Supplement Series 131, 273.
- 20. Calder AC, Fryxell B, Plewa T, Rosner R, Dursi LJ, Weirs VG, Dupont T, Robey HF, Kane JO, Remington BA, Drake RP, Dimonte G, Zingale M, Timmes FX, Olson K, Ricker P, MacNeice P and Tufo HM (2002) On validating an astrophysical simulation code. The Astrophysical Journal Supplement Series 143, 201.

 Farley DR, Shigemori K and Azechi H (2005) Laser-produced blast wave and numerical simulation using the flash code. *Laser and Particle Beams* 23, 513–519.

- 22. Tzeferacos P, Fatenejad M, Flocke N, Graziani C, Gregori G, Lamb DQ, Lee D, Meinecke J, Scopatz A and Weide K (2015) FLASH MHD simulations of experiments that study shock-generated magnetic fields. *High Energy Density Physics* 17, 24–31.
- Derouillat J, Beck A, Pérez F, Vinci T, Chiaramello M, Grassi A, Flé M, Bouchard G, Plotnikov I, Aunai N, Dargent J, Riconda C and Grech M (2018) Smilei: A collaborative, open-source, multi-purpose particle-incell code for plasma simulation. Computer Physics Communications 222, 351–373.
- 24. Arber TD, Bennett K, Brady CS, Lawrence-Douglas A, Ramsay MG, Sircombe NJ, Gillies P, Evans RG, Schmitz H, Bell AR, Ridgers CP (2015) Contemporary particle-in-cell approach to laser-plasma modelling. Plasma Physics and Controlled Fusion 57, 1–26..
- Nuckolls J, Wood L, Thiessen A and Zimmerman G (1972)Laser Compression of Matter to Super-High Densities: Thermonuclear (CTR) Applications. *Nature* 239, 139–142.
- Basov NG, Gus'kov SY and Feokistov LP (1992) Thermonuclear gain of ICF targets with direct heating of ignitor. *Journal of Soviet Laser Research* 13, 396–399.
- Haines MG (1997) Review of Inertial Confinement Fusion. Astrophysics and Space Science 256, 125–139.
- Betti R and Hurricane OA (2016) Inertial-confinement fusion with lasers. Nature Physics 12, 435–448.
- Aliverdiev A, Batani D, Dezulian R, Vinci T, Benuzzi-Mounaix A, Koenig M and Malka V (2008) Hydrodynamics of laser-produced plasma corona measured by optical interferometry. *Plasma Physics and Controlled Fusion* 50, 105013.
- Batani D, Santos J, Forestier-Colleoni P, Mancelli D, Ehret M, Trela J, Morace A, Jakubowska K, Antonelli L and del Sorbo D (2019) Optical time-resolved diagnostics of laser-produced plasmas. *Journal of Fusion* Energy 38, 299–314.
- 31. Lancaster KL, Pasley J, Green JS, Batani D, Baton S, Evans RG, Gizzi L, Heathcote R, Gomez CH, Koenig M, Koester P, Morace A, Musgrave I, Norreys PA, Perez F, Waugh JN and Woolsey NC (2009) Temperature profiles derived from transverse optical shadowgraphy in ultraintense laser plasma interactions at 6 × 10²⁰w/cm². *Physics of Plasmas* 16, 056707.
- 32. **Glenzer SH and Redmer R** (2009) X-ray thomson scattering in high energy density plasmas. *Reviews of Modern Physics* **81**, 1625–1663.
- 33. Manclossi M, Santos JJ, Batani D, Faure J, Debayle A, Tikhonchuk VT and Malka V (2006) Study of ultraintense laser-produced fast-electron propagation and filamentation in insulator and metal foil targets by optical emission diagnostics. *Physical Review Letters* 96, 125002.
- 34. Bubo M, Ren J, Wang S, Wang X, Yin S, Feng J, Wei W, Xing X, Chen B, and Zhang S (2022,) Plasma spectroscopy on hydrogen-carbon-oxygen foam targets driven by laser-generated hohlraum radiation. *Laser and Particle Beams* Volume 2022 2022 e15.
- 35. Ravasio A, Koenig M, Le Pape S, Benuzzi-Mounaix A, Park HS, Cecchetti C, Patel P, Schiavi A, Ozaki N, Mackinnon A, Loupias B, Batani D, Boehly T, Borghesi M, Dezulian R, Henry E, Notley M, Bandyopadhyay S, Clarke R, and Vinci T (2008) Hard x-ray radiography for density measurement in shock compressed matter. *Physics of Plasmas*, 15, 060701.
- 36. Morace A, Fedeli L, Batani D, Baton S, Beg FN, Hulin S, Jarrott LC, Margarit A, Nakai M, Nakatsutsumi M, Nicolai P, Piovella N, Wei MS, Vaisseau X, Volpe L and Santos JJ (2014) Development of x-ray radiography for high energy density physics. *Physics of Plasmas* 21, 102712.
- 37. Antonelli L, Atzeni S, Schiavi A, Baton SD, Brambrink E, Koenig M, Rousseaux C, Richetta M, Batani D, Forestier-Colleoni P, Bel EL, Maheut Y, Nguyen-Bui T, Ribeyre X and Trela J (2017) Laser-driven shock waves studied by x-ray radiography. *Physical Review E* 95, 063205.
- 38. Barbato F, Atzeni S, Batani D, Bleiner D, Boutoux G, Brabetz C, Bradford P, Mancelli D, Neumayer P, Schiavi A, Trela J, Volpe L, Zeraouli G, Woolsey N and Antonelli L (2019) Quantitative phase contrast imaging of a shock-wave with a laser-plasma based X-ray source. Scientific Reports 9, 18805.

- 39. Nishimura H, Mishra R, Ohshima S, Nakamura H, Tanabe M, Fujiwara T, Yamamoto N, Fujioka S, Batani D, Veltcheva M, Desai T, Jafer R, Kawamura T, Sentoku Y, Mancini R, Hakel P, Koike F and Mima K (2011) X-ray spectroscopy to study energy transport of a low-z, reduced mass target irradiated with a high-intensity laser pulse. High Energy Density Physics 7, 117–123.
- Renner O, Smid M, Batani D and Antonelli L (2016) Suprathermal electron production in laser-irradiated Cu targets characterized by combined methods of x-ray imaging and spectroscopy. *Plasma Physics and Controlled Fusion* 58, 075007.
- 41. **Morace A and Batani D** (2010) Spherically bent crystal for X-ray imaging of laser produced plasmas. *Nuclear Instruments and Methods in Physics Research Section A: Accelerators, Spectrometers, Detectors and Associated Equipment* **623**, 797–800.
- 42. Zeraouli G, Gatti G, Longman A, Pérez-Hernández JA, Arana D, Batani D, Jakubowska K, Volpe L, Roso L and Fedosejevs R (2019) Development of an adjustable Kirkpatrick-Baez microscope for laser driven x-ray sources. Review of Scientific Instruments 90, 063704.
- 43. Ducret J-E, Batani D, Boutoux G, Chance A, Gastineau B, Guillard J-C, Harrault F, Jakubowska K, Lantuejoul-Thfoin I, Leboeuf D, Loiseau D, Lotode A, Pes C, Rabhi N, Said A, Semsoum A, Serani L, Thomas B, Toussaint J-C and Vauzour B (2018) Calibration of the low-energy channel Thomson parabola of the LMJ-PETAL diagnostic sepage with protons and carbon ions. Review of Scientific Instruments 89, 023304.
- 44. Tchorz P, Szymanski M, Rosinski M, Chodukowski T and Borodziuk S (2023) Capabilities of thomson parabola spectrometer in various laser-plasma- and laser-fusion-related experiments. *Nukleonika* 68, 29–36.
- 45. Singh SK, Krupka M, Krasa J, Istokskaia V, Dostal J, Dudzak R, Pisarczyk T, Cikhardt J, Agarwal S and Klir D (2024) Hot electron emission characteristics from thin metal foil targets irradiated by terawatt laser. *Laser and Particle Beams* 42, e2.
- 46. Moore AS, Schlossberg DJ, Appelbe BD, Chandler GA, Crilly AJ, Eckart MJ, Forrest CJ, Glebov VY, Grim GP, Hartouni EP, Hatarik R, Kerr SM, Kilkenny J and Knauer JP (2023) Neutron time of flight (nToF) detectors for inertial fusion experiments. Review of Scientific Instruments 94, 061102.
- Slutz SA, Herrmann MC, Vesey RA, Sefkow AB, Sinars DB, Rovang DC, Peterson KJ and Cuneo ME (2010) Pulsed-power-driven cylindrical liner implosions of laser preheated fuel magnetized with an axial field. *Physics of Plasmas* 17, 056303.
- 48. **Slutz SA and Vesey RA** High-Gain Magnetized Inertial Fusion. *Physical Review Letters* **025003**, 1–5.
- 49. Slutz SA, Gomez MR, Hansen SB, Harding EC, Hutsel BT, Knapp PF, Lamppa DC, Awe TJ, Ampleford DJ, Bliss DE, Chandler GA, Cuneo ME, Geissel M, Glinsky ME, Harvey-Thompson AJ, Hess MH, Jennings CA, Jones B, Laity GR, Martin MR, Peterson KJ, Porter JL, Rambo PK, Rochau GA, Ruiz CL, Savage ME, Schwarz J, Schmit PF, Shipley G, Sinars DB, Smith CI, Vesey RA and Weis MR Enhancing performance of magnetized liner inertial fusion at the Z facility. Physics of Plasmas 25, 112706.
- Zakharov SM, Ivanenkov GV, Kolomenskij AA, Pikuz SA, Samokhin AI and Ulshmid I (1982) Wire x-pinch in a high-current diode. *Pis'ma v Zhurnal Tekhnicheskoj Fiziki* 8, 1060–1063.
- 51. Nissim N, Greenberg E, Werdiger M, Horowitz Y, Bakshi L, Ferber Y, Glam B, Fedotov-Gefen A, Perelmutter L and Eliezer S (2021) Freesurface velocity measurements of opaque materials in laser-driven shockwave experiments using photonic doppler velocimetry. Matter and Radiation at Extremes 6, 046902.
- 52. Boutoux G, Chevalier J-M, Arrigoni M, Berthe L, Beuton R, Bicrel B, Galtie A, Hébert D, Clanche JL, Loillier S, Loison D, Maury P, Raffray Y and Videau L (2023) Experimental evidence of shock wave measurements with low-velocity (< 10 m/s) and fast dynamics (< 10 ns) capabilities using a coupled photonic doppler velocimetry (pdv) and triature velocity interferometer system for any reflector (visar) diagnostic. Review of Scientific Instruments 94, 033905.</p>
- Strand OT, Goosman DR, Martinez C, Whitworth TL and Kuhlow WW (2006) Compact system for high-speed velocimetry using heterodyne techniques. Review of Scientific Instruments 77, 083108.

- Al'tshuler LV, Kormer SB, Bakanova AA and Trunin RF (1960) Equation of state for aluminum, copper, and lead in the high-pressure region. Sov. Phys. JETP 11, 573.
- 55. Mitchell AC, Nellis WJ, Moriarty JA, Heinle RA, Holmes NC, Tipton RE and Repp GW (1991) Equation of state of Al, Cu, Mo, and Pb at shock pressures up to 2.4 Tpa (24 Mbar). Journal of Applied Physics 69, 2981–2986.
- Barker LM and Hollenbach RE (1972) Laser interferometer for measuring high velocities of any reflecting surface. *Journal of Applied Physics* 43, 4669–4675.
- Barker LM and Schuler KW (1974) Correction to the velocity-per-fringe relationship for the visar interferometer. *Journal of Applied Physics* 45, 3692–3693.
- 58. **Bloomquist DD and Sheffield SA** (1983) Optically recording interferometer for velocity measurements with subnanosecond resolution. *Journal of Applied Physics* **54**, 1717–1722.
- Celliers PM, Bradley DK, Collins GW, Hicks DG, Boehly TR and Armstrong WJ (2004) Line-imaging velocimeter for shock diagnostics at the omega laser facility. Review of Scientific Instruments 75, 4916–4929.
- Bolme CA and Ramos KJ (2013) Line-imaging velocimetry for observing spatially heterogeneous mechanical and chemical responses in plastic bonded explosives during impact. Review of Scientific Instruments 84, 083903.
- Ramis R, Schmalz R and Meyer-Ter-Vehn J (1988) Multi a computer code for one-dimensional multigroup radiation hydrodynamics. *Computer Physics Communications* 49, 475–505.

- 62. T4 Group LANL. EOS SESAME tables developed at the Los Alamos laboratory (SESAME report on the Los Alamos equation-of- state library, report no. LALP-83-4, 1983, and report LA-UR-92-3407, 1992, T4 group LANI, Los Alamos). Report LA-UR-92-3407, 1992.
- 63. More RM, Warren KH, Young DA and Zimmerman GB (1988) A new quotidian equation of state (QEOS) for hot dense matter. *The Physics of Fluids* 31, 3059–3078.
- For more information on PrOpacEOS, visit:. https://www.prism-cs.com/ Software/Propaceos/overview.html.
- 65. Delettrez J, Epstein R, Richardson MC, Jaanimagi PA and Henke BL (1987) Effect of laser illumination nonuniformity on the analysis of time-resolved x-ray measurements in UV spherical transport experiments. *Physical Review A* 36, 3926–3934.
- 66. Bardy S, Aubert B, Bergara T, Berthe L, Combis P, Hebert D, Lescoute E, Rouchausse Y and Videau L (2020) Development of a numerical code for laser-induced shock waves applications. Optics & Laser Technology 124, 105083
- Larsen JT and Lane SM (1994) Hyades—a plasma hydrodynamics code for dense plasma studies. *Journal of Quantitative Spectroscopy and Radiative Transfer* 51, 179–186.
- Ramis R and Meyer ter Vehn J, and Ramirez J (2009) Multi2d a computer code for two-dimensional radiation hydrodynamics. Computer Physics Communications, 180, 977–994.
- Amit G, Mosseri I, Even-Hen O, Schneider N, Fisher E, Datz H, Cohen E, and Nissim N (2022) Particles detection system with cr-39 based on deep learning. Laser and Particle Beams Volume 2022 2022 e12.